Journal of Atmospheric and Solar-Terrestrial Physics 75-76 (2012) 147–160

Contents lists available at SciVerse ScienceDirect

Journal of Atmospheric and Solar-Terrestrial Physics

journal homepage: www.elsevier.com/locate/jastp

Dynamical amplification of the stratospheric solar response simulated with the Chemistry-Climate Model LMDz-Reprobus

M. Marchand [a,b,c,*], P. Keckhut [a,b,c], S. Lefebvre [a,b,c], C. Claud [d], D. Cugnet [a,b,c], A. Hauchecorne [a,b,c], F. Lefèvre [a,b,c], M.-P. Lefebvre [f], J. Jumelet [a,b,c], F. Lott [e], F. Hourdin [f], G. Thuillier [a,b,c], V. Poulain [a,b,c], S. Bossay [a,b,c], P. Lemennais [a,b,c], C. David [a,b,c], S. Bekki [a,b,c]

[a] Université Versailles St-Quentin, France
[b] UPMC Université Paris, France
[c] CNRS/INSU, LATMOS-IPSL, Tour 45-46/3ème étage, 4 place Jussieu, 75252 PARIS cedex 05, France
[d] LMD/IPSL, Ecole Polytechnique, 91128 Palaiseau Cedex, France
[e] LMD/IPSL, 24, rue Lhomond, 75231 Paris Cedex 05, France
[f] LMD/IPSL, UPMC, Tour 45-55, 4 place jussieu 75005 Paris, France

ARTICLE INFO

Article history:
Received 31 December 2010
Received in revised form
16 October 2011
Accepted 17 November 2011
Available online 10 December 2011

Keywords:
Solar
Chemistry Climate Model
Dynamics
Stratosphere
SSW

ABSTRACT

The impact of the 11-year solar cycle on the stratosphere and, in particular, on the polar regions is investigated using simulations from the Chemistry Climate Model (CCM) LMDz-Reprobus. The annual solar signal clearly shows a stratospheric response largely driven by radiative and photochemical processes, especially in the upper stratosphere. A month-by-months analysis suggests that dynamical feedbacks play an important role in driving the stratospheric response on short timescales. CCM outputs on a 10 days frequency indicate how, in the northern hemisphere, changes in solar heating in the winter polar stratosphere may influence the upward propagation of planetary waves and thus their deposition of momentum, ultimately modifying the strength of the mean stratospheric overtuning circulation at middle and high latitudes. The model results emphasize that the main temperature and wind responses in the northern hemisphere can be explained by a different timing in the occurrence of Sudden Stratospheric Warmings (SSWs) that are caused by small changes in planetary wave propagation depending on solar conditions. The differences between simulations forced by different solar conditions indicate successive positive and negative responses during the course of the winter. The solar minimum simulation generally indicates a slightly stronger polar vortex early in the winter while the solar maximum simulation experiences more early SSWs with a stronger wave-mean flow interaction and reduced zonal wind at mid-latitudes in the upper stratosphere. The opposite response is observed during mid-winter, in February, with more SSWs simulated for solar minimum conditions while solar maximum conditions are associated with a damped planetary wave activity and a reinforced vortex after the initial stratospheric warming period. In late winter, the response is again reversed, as noticed in the temperature differences, with major SSW mostly observed in the solar maximum simulation and less intense final warmings simulated for solar minimum conditions. Due to the non-zonal nature of SSWs, the stratospheric response presents high regional variability during the northern hemisphere winter. As a result, successive positive and negative responses are observed during the course of the winter.

1. Introduction

The Earth climate is primarily driven by the sun. The discussion, about the potential contribution of the sun fluctuations on the climate evolution, requires an improvement of our knowledge on the origin and mechanisms of the solar forcing. Solar activity disturbances on different time-scales can affect our atmosphere in many different ways (Haigh, 2007; Gray et al., 2010). There are several properties of the sun emissions that vary and may contribute to atmospheric and climate change on Earth: Total Solar Irradiance (TSI) changes, variations in the ultraviolet part of the solar spectrum, and varying energetic electron and proton precipitations. The change in TSI over the 11-year cycle from solar minimum to solar maximum is only of 0.1%. About a third of the TSI change over the 11-year solar cycle occurs below 250 nm

* Corresponding author at: UPMC Université Paris, France.
Tel.: +33 144273221; fax: +33 144273776.
E-mail address: marion.marchand@latmos.ipsl.fr (M. Marchand).

1364-6826/$ - see front matter © 2011 Elsevier Ltd. All rights reserved.
doi:10.1016/j.jastp.2011.11.008

(Lean, 1989). The UV radiation fluctuations can induce significant atmospheric variability through changes in absorption by O_3 and O_2 and photochemistry, primarily in the middle to upper stratosphere at low latitudes (Haigh, 1994). A plausible mechanism for solar influences on the atmosphere, therefore, might invoke changes in stratospheric temperature and ozone due to ultraviolet (UV) variations. In addition, transport-induced changes in ozone can occur as a consequence of indirect effects on circulation caused by the above process (Hood and Soukharev, 2003; Rind et al., 2004; Shindell et al., 2006; Gray et al., 2009). Variations in both ozone and temperature in the stratosphere have been linked successfully to solar cycles using observations and model simulations (Gray et al., 2010). Chemistry models imposing idealized ozone changes reproduced the temperature response especially the maximum warming around the equatorial stratopause (Haigh, 1999; Shindell et al., 1999, 2001; Larkin et al., 2000; Rind, 2002; Matthes et al., 2003; Haigh, 2003). Nonetheless, large unexplained differences between the calculated and observed stratospheric response persist such as the observed poleward and downward propagation of the signal at polar latitudes (Matthes et al., 2003), the negative temperature response at high latitudes (Keckhut et al., 2005), or the secondary maximum in the equatorial lower stratosphere. The quantification of the atmospheric response due to solar changes requires more sophisticated numerical models such as Chemistry Climate Models (CCMs) that describe all the required stratospheric photochemistry, radiative and dynamical processes and their interactions in both the troposphere where waves are generated and in the middle atmosphere where waves propagate and dissipate. Studies using these models showed a real improvements of the vertical structure of the annual mean ozone signal in the tropics, including the lower stratospheric maximum even if the peak in the upper stratosphere tends to be slightly lower than observed (Labitzke et al., 2002; Tourpali et al., 2003; Egorova et al., 2004; Rozanov et al., 2004; Shindell et al., 2006; Schmidt and Brasseur, 2006; McCormack et al., 2007; Marsh et al., 2007; Austin et al., 2007, 2008; Matthes et al., 2007, 2010). The direct effect of the 11-year solar cycle on ozone via radiation and chemistry in the upper stratosphere depends generally on a good representation of solar radiation processes in both the radiative transfer and in the photochemistry parameterisation (see Chapters 3 and 6 in SPARC-CCM Val Report, 2011 and Forster et al., 2011). However, the indirect dynamical effect in the tropical lower stratosphere and extra-tropical stratosphere and the extension of the signal into the troposphere (Gray et al., 2010) are more challenging to reproduce. These studies highlighted the importance of different factors such as realistic interannual variability in the SSTs variables, the time-varying solar cycle or the QBO in the stratospheric solar response. Hence, despite these general improvements in our understanding of mechanisms involved in the atmospheric solar response, there are still specific features that are not reproduced by models especially in polar regions.

The initial UV-driven changes in heating rate and ozone, although small, could induce significant dynamical changes on a global scale (Hines, 1974). Observations and analyses have indeed reported large dynamical signatures in the middle atmosphere at high latitudes correlated with solar activity, which tend to support this idea. Indeed, a solar temperature anomaly near the equatorial stratopause could induce wind anomalies and therefore influence the propagation of planetary waves in the winter hemisphere (Kodera, 1995)Thus, changes in the planetary wave forcing could play an important role in the dynamical feedbacks (Chandra, 1986; Gray et al., 2001; Kodera and Kuroda, 2002), especially by influencing the strength of the large-scale Brewer–Dobson (B–D) circulation that may be transferred and may amplify the atmospheric solar signal from the equatorial stratopause to the lower polar stratosphere. Mechanistic simulations (Hampson et al., 2006) have shown that the atmospheric response at high latitudes is not a linear function of the solar forcing and depends on the background level of wave activity, triggering polar stratospheric warming events. Such large dynamical events can have the potential to cause anomalies in the stratospheric circulation that can propagate to the surface (Baldwin et al., 2003).

In this paper, we investigate the middle atmospheric response to the 11-year solar cycle using the fully interactive 3D coupled Chemistry-Climate Model LMDz-Reprobus (Jourdain et al., 2008) especially in polar region. Our focus is the relationship between the stratospheric solar response and the occurrence of the stratospheric warming and their timing during the course of the winter. Since these dynamical processes are difficult to detect from a Multi Linear Regression (MLR) analysis of transient simulation, the CCM used here was integrated for two 30-year time slices representative of solar maximum and solar minimum conditions. Comparisons between the two simulations are used to derive the stratospheric response to solar forcing. In this approach, all external forcings are identical in both simulations except for the solar irradiance; the solar forcing is also kept constant in time in each simulation allowing to focus our analysis only on the relationship between the atmospheric solar response and the dynamical polar processes. It is worth keeping in mind that this model set up might tend to amplify slightly the atmospheric response to solar changes and is less comparable to solar signals derived from observations where obviously the solar forcing is time varying. We investigated the atmospheric response in monthly—but also over 10 days time scale—means, particularly for high latitudes. The paper is organised as follows. Section 2 provides a description of LMDz-Reprobus CCM and the experimental setup. The third section shows the solar signature in ozone, temperature and wind fields in the LMDz-Reprobus simulations. Section 4 describes the role of the dynamics in the amplification of the solar signal and Section 5 provides results on the northern hemispheric longitudinal response. A summary of the results and main conclusions are presented in Section 6.

2. Model description

The LMDz-Reprobus model is a Chemistry-Climate Model based on the coupling between LMDZ4 general circulation model (Sadourny and Laval, 1984; Le Treut et al., 1994, 1998; Hourdin et al., 2006) and the Reprobus stratospheric chemistry package (Lefèvre et al., 1994, 1998). The model extends from the ground up to 65 km, on 50 hybrid σ-pressure vertical levels (Lott et al., 2005). The resolution in the stratosphere varies from about 1 km at an altitude of 12 km to 3 km at 50 km. For the applications presented here, the model was integrated with a horizontal resolution of 3.75° in longitude and 2.5° in latitude.

A first version of LMDz-Reprobus has been extensively described by Jourdain et al. (2008). Since that study, an important improvement brought to the underlying GCM physics (LMDZ4) is the replacement of the Tiedtke (1989) convection scheme by that described in Emanuel (1991, 1993). This change has been shown by Hourdin et al. (2006) to lead to a better representation of the large-scale tropospheric dynamics. It also has the interesting effect of improving the temperature climatology of the model in the lower stratosphere. In particular, the use of the Emanuel (1991) convection scheme in LMDz-Reprobus reduces significantly the cold bias previously noted in the polar stratosphere in winter–spring (Jourdain et al., 2008).

The Reprobus chemistry module is basically unchanged from the version used by Jourdain et al. (2008). It includes 55 chemical species and a comprehensive description of the stratospheric chemistry. Absorption cross-sections and kinetics data are based

on the latest JPL recommendation (Sander et al., 2006). The monthly varying global distribution of background (e.g. non-volcanic) stratospheric sulphuric acid aerosol is provided by a two-dimensional model long-term simulation (Bekki et al., 1993) for the 2000 year ensuring that the seasonal variation of the background aerosol levels is typical of the last 11-year solar cycle. The heterogeneous chemistry included in the model takes into account the reactions on binary and ternary liquid aerosols, as well as on solid NAT or on water-ice particles. The irreversible vertical transfer of HNO_3 and H_2O due to the sedimentation of PSCs (i.e. denitrification) is also taken into account. In the troposphere, where the chemistry is not explicitly treated by Reprobus, the model is relaxed towards a monthly varying climatology of O_3, CO, and NO_x computed by the TOMCAT chemical-transport model (Law et al., 1998; Savage et al., 2004).

The photolysis rates used in Reprobus are pre-calculated off-line with the Tropospheric and Ultraviolet visible (TUV) model (Madronich and Flocke, 1999). TUV calculates in spherical geometry the actinic flux, scattering, and absorption through the atmosphere by the multistream discrete ordinate method of Stamnes et al. (1988). The spectral domain covers the 116–850 nm interval. Calculations of photolyse rate are performed on a 1 nm wavelength grid, except in the regions of importance for the 11-year solar cycle, where the resolution is largely increased to accurately describe the spectral features in the solar flux or in the absorption cross-sections: the wavelength resolution of our calculations with TUV reaches 0.01 nm in the Schumann–Runge bands of O_2. At this resolution, the absorption by O_2 in the Schumann–Runge bands can be computed line-by-line, and we used for that purpose the temperature-dependent polynomial coefficients determined by Minschwaner et al. (1992). The temperature dependence of absorption cross-sections is taken into account using climatological temperature profiles. The albedo considered for the computation of photolysis rates is set to a globally averaged value of 0.3 with solar zenith angle varying from 0 to 95°. Once calculated, the photolysis rates of the 36 species photodissociated in LMDz-Reprobus are stored in a 3-dimensional look-up table as a function of the overhead O_2 column, the overhead O_3 column, and the solar zenith angle. For each sunlit grid point, the actual photolysis rates used by LMDz-Reprobus are then interpolated in the table according to those three parameters.

We perform 30-years integrations of the Chemistry-Climate Model for solar maximum versus solar minimum conditions. Four years being taken as spin up, the results presented here are based on the last 26 years of simulation. For each of the two experiments, the solar spectra used to compute the photolysis rates between 116 and 410 nm were specified from the measurements of the SUSIM instrument on board the UARS satellite (Floyd et al., 2003). These data were obtained respectively on 2 February 1992 (solar maximum) and 10 October 1996 (solar minimum) (see Figs. 1 and 2). The difference between the two measured solar spectra used in the forcing of the simulations (5% for the 200–250 nm band) is larger than the commonly used difference found between the maximum and minimum of a typical 11 year cycle that is derived from monthly averaged reconstructed spectra (3.5% for the 200–250 nm band). At longer wavelengths (410–850 nm), where the variability of the solar flux over the 11-year cycle is negligible, we used for both simulations the same spectrum measured in March 1992 by the SOLSPEC instrument on the Space Shuttle (Thuillier et al., 2004).

The solar part of the radiative scheme is based on an improved version of the two bands scheme developed by Fouquart and Bonnel (1980) and the thermal infrared part of the radiative code is taken from Morcrette et al. (1986). While this scheme is crude, note that the thermal component of the solar forcing (e.g. changes in net heating from solar changes only, keeping chemical composition unchanged) does not exhibit a dependency on wavelength as strong as the photolysis component of the solar forcing. Nonetheless,

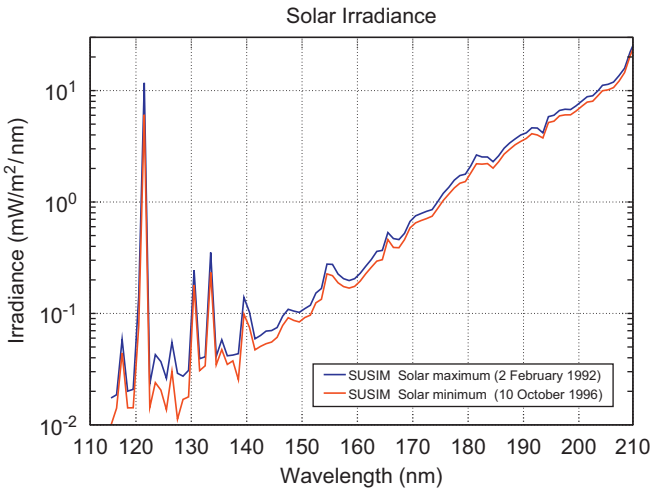

Fig. 1. Variation of the composite solar spectrum for the chosen dates February 2, 1992 and October 10, 1996.

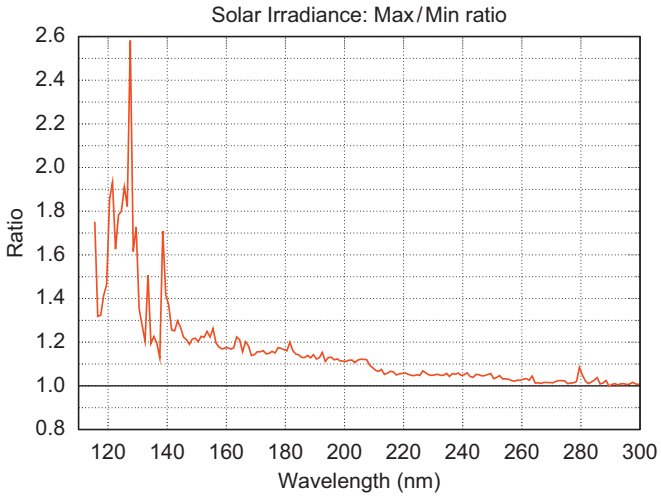

Fig. 2. Ratio between maximum and minimum of the solar cycle signals.

the use of a simple two bands radiation code tends to underestimate the temperature response when compared to other radiation models with the same solar irradiance fluctuations (SPARC-CCM Val Report, 2011; Forster et al., 2011). The radiative scheme takes into account the radiatively active species H_2O, CO_2, O_3, N_2O, CH_4, CFC-11, and CFC-12. Surface mixing ratios for these constituents are identical for both GCM experiments, and are constrained by values typical of the year 2000 (scenario REF-B1 of Eyring et al., 2008).

Finally, the sea surface temperature and sea ice concentration used in both simulations are forced by the same AMIP (Atmospheric Model Intercomparison Project) climatology (Kanamitsu et al., 2002) averaged over the 1995–2004 period and the QBO is not generated in our model.

3. Atmospheric response to solar forcing

3.1. Annual ozone and temperatures solar signature

The 11-year solar cycle has a direct impact on ozone via radiation (thermal effect) and photochemistry (photolysis effect), especially in the upper stratosphere, and an indirect impact through dynamics and transport and coupling with chemistry throughout the stratosphere (Gray et al., 2010). Fig. 3 presents the model-simulated annual mean

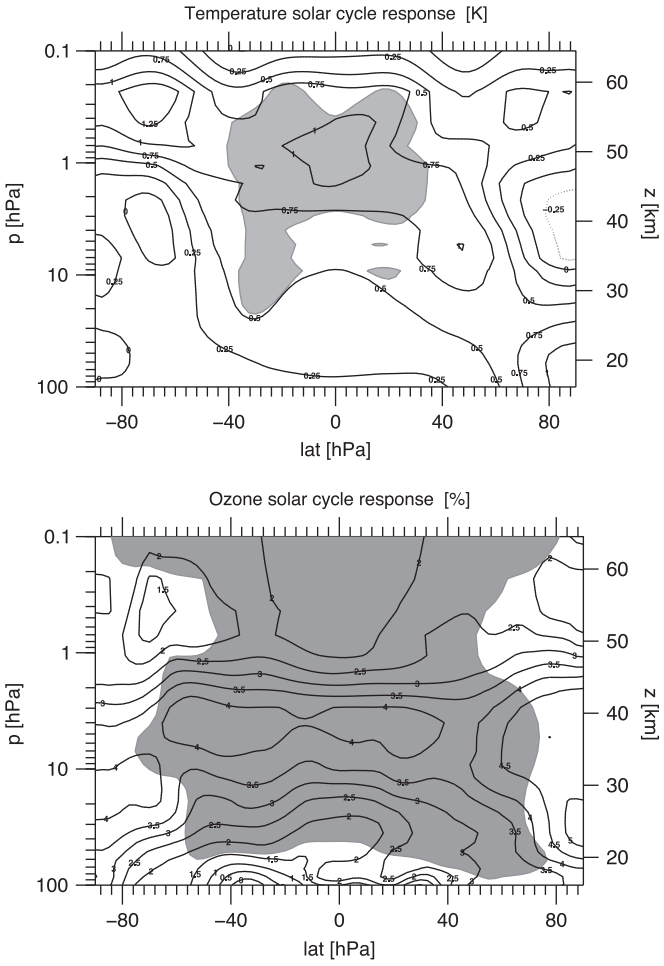

Fig. 3. Annual climatology (over 26 years of simulation) of temperature and ozone response (%) over a 11-year solar cycle (difference between solar maximum and minimum conditions) as a function of pressure and latitude.

(averaged over the 26 years of simulation) changes in temperature and ozone mixing ratio between the solar maximum and solar minimum conditions. The shade of grey corresponds to 90% significance level. A statistically significant solar signal is obtained only in middle and upper stratosphere of the low and mid-latitudes, and in the tropical lower stratosphere.

The largest temperature and ozone solar response occurs in the upper stratosphere between 1 and 3 hPa. This is mostly caused by the direct solar effect (thermal and photolysis effect) which is initiated by enhanced UV absorption during solar maxima that leads to higher temperatures and greater ozone through enhanced photochemical production from the O_2 photolysis, which in turn increases the temperature.

In our study, the model produces a tropical temperature response of about 1 K around the stratopause and 0.3 K below 10 hPa, corresponding to 0.77 K and 0.23 K per 100 units of the F10.7 cm radio flux respectively; the last set of values are provided in order to facilitate the comparison with other studies. Note that the direct comparison remains difficult because the 11-year solar cycle amplitude itself exhibits a very significant variability from one cycle to another.

The temperature difference between solar maximum and minimum is significantly positive in most parts of the stratosphere extending downward from the tropical stratopause over mid-latitudes with a signal more pronounced in the northern hemisphere. A vertical dipolar structure appears in the temperature response for higher latitudes in the HN, with a positive signal in the upper stratosphere and a negative signal in the middle stratosphere. However, this response is not statistically significant due to the large interannual variability.

The temperature response from fixed phase solar forcing simulations tends to be slightly larger than results from transient simulation of the same model (0.6 K and 0.1 K per 100 units of the F10.7 cm radio flux at the stratopause and below 10 hPa respectively, SPARC-CCM Val Report, 2011). This is typical of model studies based on simulations forced by constant solar maximum and minimum conditions respectively. In our case, this effect should be even more pronounced because the difference between the measured solar spectra used as inputs to the model are larger than the difference between the maximum and the minimum of a typical 11-years solar cycle reconstructed monthly mean solar spectra and used to force a transient simulation of our model (SPARC-CCM Val Report, 2011). The solar response deduced from this transient simulation of LMDz-Reprobus has been compared against measurements and other CCMs in the framework of the CCMVal Activity of SPARC-CCM Val Report (2011). The LMDZ-Reprobus temperature response appears to be within the lower range of the response of the other CCMs (1.1–0.35 K) in the upper stratosphere. This under-estimation of the shortwave heating in our model is certainly due to the low spectral resolution (two bands) of the radiation code. While the majority of the modelled upper stratospheric temperature responses seen in the CCMs are broadly similar to the solar signal seen in SSU observations (Randel et al., 2009), discrepancies between the models themselves and with observations sharply increase below 10 hPa. Some CCMs like LMDz-Reprobus show a positive solar temperature signal that increases with increasing height, which is in good agreement with SSU data (Randel et al., 2009). Other models show a relative minimum in the middle stratosphere like the one derived from ERA-40 data (Uppala et al., 2005) and some models show a distinct temperature maximum in the lower stratosphere which is present in the RICH radiosonde (Haimberger et al., 2008) and ERA-40 data (Uppala et al., 2005).

Enhanced solar irradiance yields a statistically significant ozone increase in the stratosphere, mainly because of the faster oxygen photolysis. The vertical structure of the ozone response derived from the difference between our two constant solar min and max simulations (Fig. 3) shows a maximum of 4% at about 35–40 km. This response is larger than the response derived from a transient simulation performed with the same model (SPARC-CCM Val Report, 2011). This is mainly due to the larger difference between the measured min and max solar spectra used here compared to the amplitude of the average solar cycle used in the transient simulation (SPARC-CCM Val Report, 2011), as mentioned earlier. Interestingly, when considering the solar response in temperature, this overestimation of the ozone response somewhat also compensates for the underestimation of shortwave heating in our model originating from the low spectral resolution of the radiative code. Similar to the rather good agreement on the vertical structure of the solar signal in temperature, the evaluation of transient simulations in SPARC-CCM Val Report (2011) found that the ozone response in CCMs compare well with the one derived from Randel and Wu (2007) ozone data in the middle and upper stratosphere; however, the agreement between models, and between the models and observations deteriorates in the lower stratosphere due to the increased uncertainties. One can notice that NIWA-3D data (Hassler et al., 2009) set shows a vertical structure of the ozone response that differs from the Randel and Wu ozone data especially in the lower stratosphere with a secondary peak in ozone between 20 and 25 km (region where the largest ozone column changes occur) which is simulated in some of the CCMs (SPARC-CCM Val Report, 2011). The LMDz-Reprobus ozone response (derived from the

present fixed phase solar forcing simulations or from the transient simulations) exhibits a very small secondary peak in the lower stratosphere which is found much lower than in the Randel and Wu (2007) ozone data. There is general consensus that this secondary maximum in the equatorial lower stratosphere results from transport processes. In particular, it is associated to solar-induced changes in planetary wave forcing, and hence changes in the strength of the large-scale Brewer–Dobson circulation that seems to be underestimated in the LMDz-Reprobus CCM.

3.2. Seasonal ozone solar signature

The climatological ozone response derived from the difference between the solar maximum and minimum simulations as a function of pressure and month is shown in Fig. 4 for low (15°S–15°N) and high latitudes (70°N–90°N, 90°S–70°S). As expected, the largest effect (5%) seen in the tropical band (associated with two maxima in March and in October) corresponds to both equinoxes when the solar average zenith angle is the smallest (Fig. 4a). These two statistically significant maxima in the ozone response are located at 40 km in good agreement with previous 2D photochemical simulations (Brasseur, 1993) and 3D model simulations (Austin et al., 2008). The amplitude of the ozone response in the tropical stratosphere observed at the 11-year time scale range values between 2% and 4% and is in good agreement with our results described here. However, direct comparisons with observations are difficult to analyse because the solar cycle amplitude itself exhibit a large variability (factor of nearly 2) from one cycle to another and even more on the scale of solar-rotation and, the atmosphere response derived from observations depends on the multi-linear regression analysis. At high latitudes, the amplitude of the climatological ozone response can be two or three times larger than the tropical one during winter–spring months (Fig. 4b,c). Even if the inter-annual variability is large during these months, the response remains relatively significant. The two Hemispheres exhibit slightly different responses. In the upper stratosphere Northern Hemisphere (NH), the difference between maximum and minimum solar conditions shows a positive ozone anomaly in January followed by a negative one in February. In contrast, in the upper stratosphere of the Southern Hemisphere (SH) known to be less perturbed dynamically, smaller differences on ozone fields as well as temperature anomalies are simulated in winter. In the lower stratosphere where the horizontal transport dominates, we observe an increase of ozone in January in NH. In the Southern Hemisphere, we observe an ozone increase in October followed by an ozone decrease in December that appear not statistically significant. At mid-latitudes (not shown) the response is more complex because it results from the mixing of the low and high latitudes ozone signals. It includes both the photochemical effect as observed in the tropical band with smaller amplitudes as expected, and a dynamical feedback in NH winter in both the upper stratosphere and in the vicinity of the tropopause.

3.3. Seasonal temperature solar signature

The climatological temperature response derived from the difference between the solar maximum and minimum simulations as a function of pressure and month for low and high latitude bands (same as in Fig. 4) is shown in Fig. 5. In low latitudes, the response in the upper stratosphere (above 1 hPa) is positive and is maximum (minimum) during winter (summer)

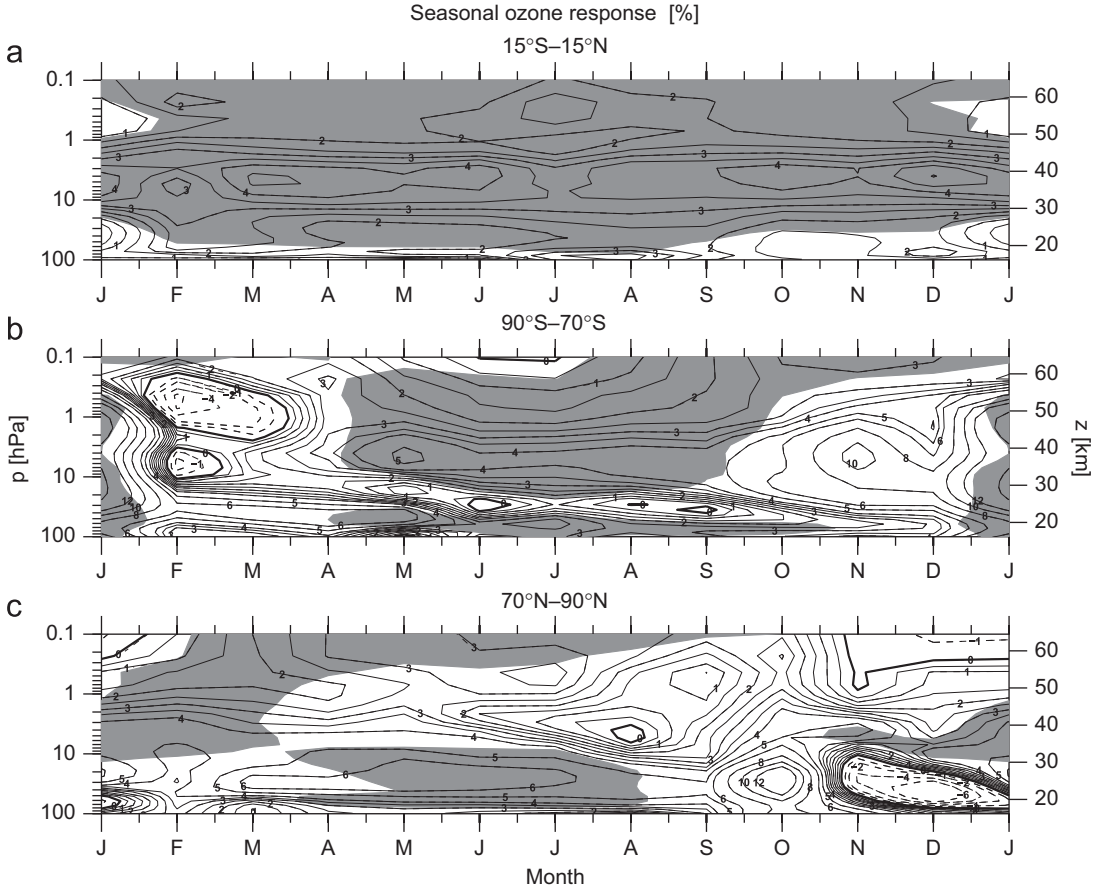

Fig. 4. Monthly climatology (over 26 years of simulation) of ozone response (%) over a 11-year solar cycle (difference between solar maximum and minimum conditions), as a function of pressure for 15°S–15°N, 90°S–70°S, 70°N–90°N latitude bands.

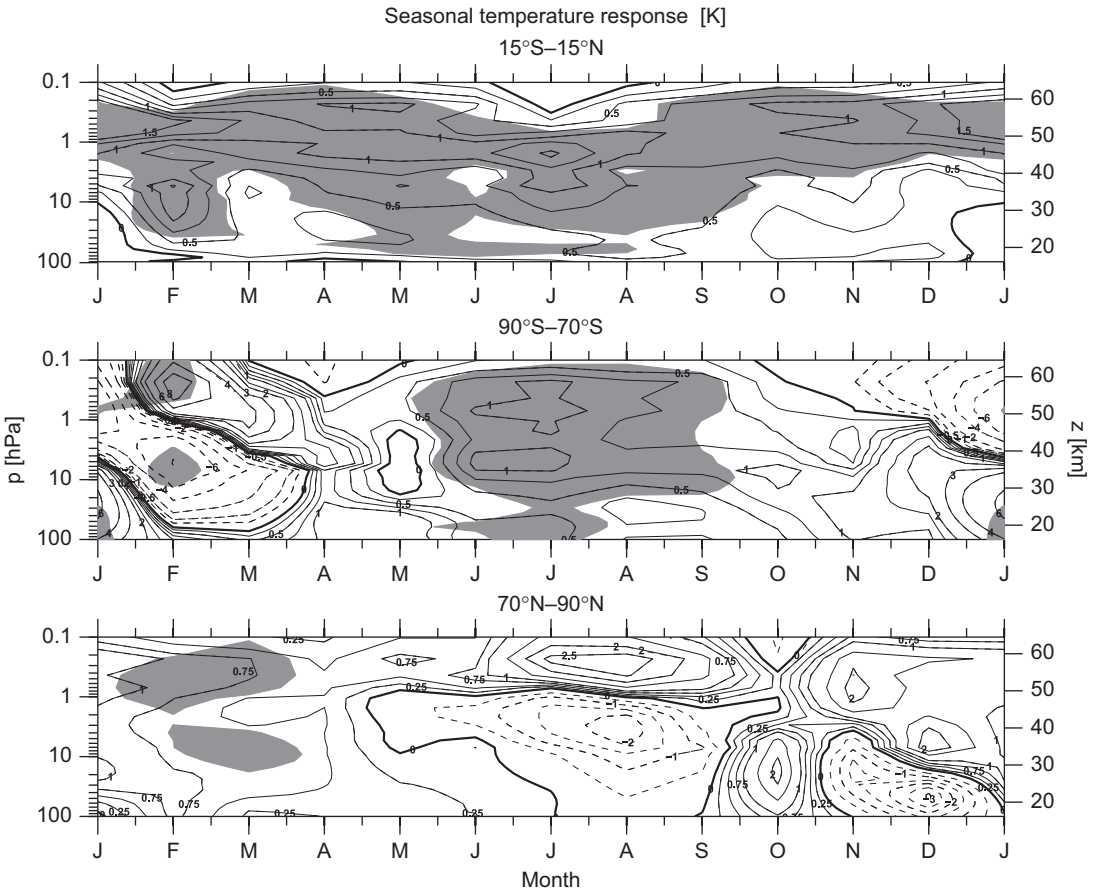

Fig. 5. Monthly climatology (over 26 years of simulation) of temperature response (K) over a 11-year solar cycle (difference between solar maximum and minimum conditions), as a function of pressure for 15°S–15°N, 90°S–70°S, 70°N–90°N latitude bands.

months. In the low stratosphere, the tropical response is larger in JJA, in agreement with observations (Claud et al., 2008), but also in February–March, in relationship with the opposite response at high latitudes (see below). For high latitudes, the temperature response to the 11-year solar cycle is of larger amplitude (5–10 K) and is strongly correlated with ozone anomalies as suggested by the comparison between Figs. 4 and 5. In the Northern Hemisphere low stratosphere, the temperature response is positive during early winter, and negative during late winter and is related to a weaker and a stronger polar vortex respectively (see next section). The response is opposite in the middle and upper stratosphere. In the Southern Hemisphere, the temperature response is negative in the 10–1 hPa pressure range, associated with a stronger polar vortex, and positive above. This is expected because the strong planetary wave activity can result in anti-correlated perturbations in these two regions (Hauchecorne and Chanin, 1983). In the lower stratosphere, a positive response during SON followed by a negative response during NDJ are observed, positively correlated with the ozone response. This structure appears, however, not statistically significant.

3.4. Zonal wind solar signature

The climatological zonal wind response derived from the difference between the solar maximum and minimum simulations as a function of pressure and month for low (15°S–15°N) and mid-high latitude bands (50°N–70°N, 70°S–50°S) is shown in Fig. 6. In low latitudes, below 5 hPa, the response of zonal winds to solar forcing is rather weak: the zonal winds are generally slightly weaker in case of high solar activity, with the exception of the upper stratosphere from December until April. In the Northern Hemisphere mid- and high-latitudes, a substantial response of the zonal wind to the solar forcing appears during winter: zonal winds decrease in early winter, and increase in late winter. This response is consistent with the temperature response, with a polar vortex weaker at the beginning of the winter and stronger afterwards. In the Southern Hemisphere, for high-latitudes, zonal winds, in case of solar maximum, increase during winter months, decrease in October and then increase from November onwards. However, the zonal wind solar signature tends to be not statistically significant.

4. Role of the dynamics

4.1. Potential mechanisms

With a tropical stratospheric response to solar forcing in our simulations that agrees well with previous numerical models and the expected photochemical effects, the response at high and mid-latitudes exhibits large amplitude disturbances in ozone, temperature and wind that provide coherent patterns. In the upper stratosphere, mainly in the tropical band (Fig. 4a) where solar forcing is expected to be maximum, ozone increases due to oxygen photo-dissociation and temperatures increase because of ozone solar absorption. This effect is damped due to the temperature dependence of the Chapman cycle (Keating et al., 1987). Such temperature increases, even of small amplitude, modify the meridional gradients in temperature and zonal winds, and therefore modulate the propagation of planetary waves (Kodera and Kuroda, 2002). The large atmospheric differences at mid-high

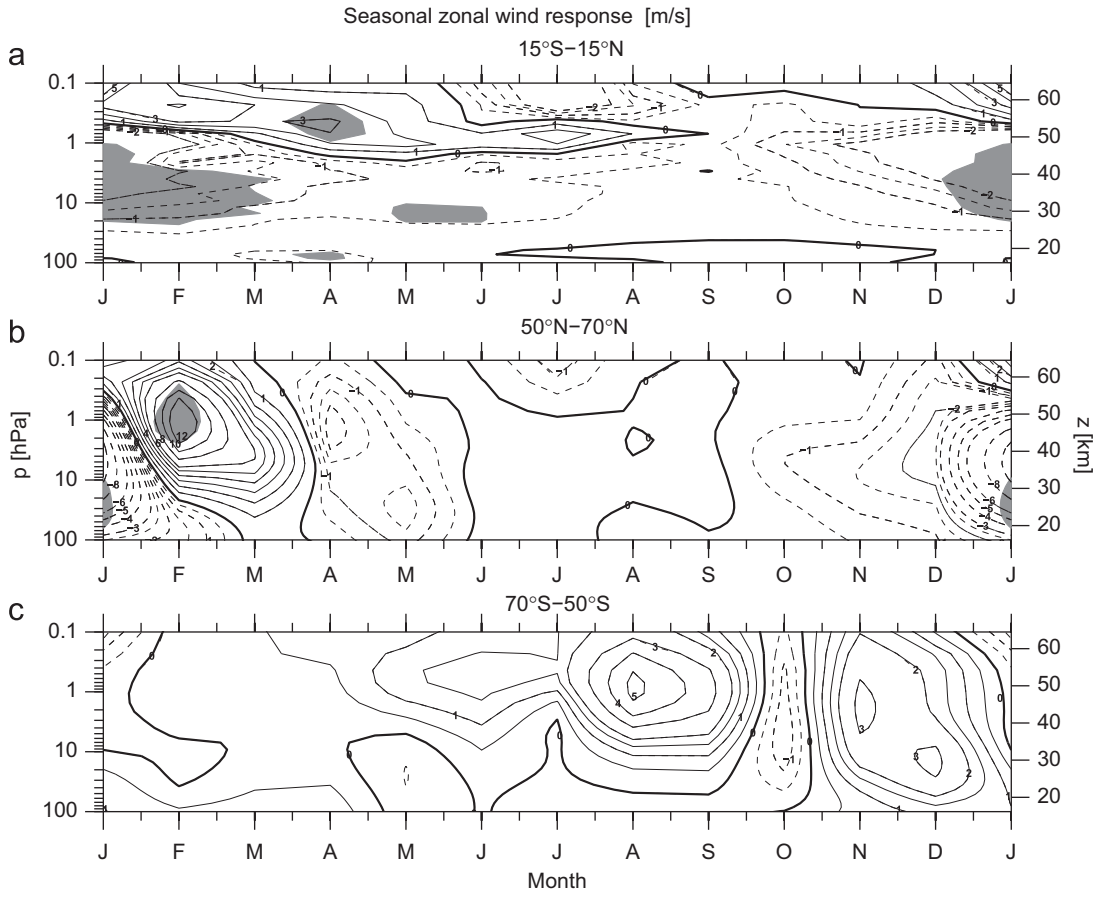

Fig. 6. Monthly climatology (over 26 years of simulation) of zonal wind response (m s^{-1}) over a 11-year solar cycle (difference between solar maximum and minimum conditions), as a function of pressure for 15°S–15°N, 70°S–50°S, 50°N–70°N latitude bands.

latitudes between solar maximum and minimum conditions cannot be explained by radiative and photodissociation processes only. This supports the idea of a significant contribution of dynamics in the solar stratospheric response. Atmospheric waves at different scales have the potential to link different regions vertically and horizontally and to bring energy momentum far from their sources. The atmospheric background (3D temperature and wind field) has a large impact on wave propagation, mean flow, and air mass circulation. In principle, this mechanism was proposed long time ago (Hines, 1974). This mechanism was difficult to test until recently since meteorological analyses were not available up to the stratosphere and numerical tools not enough sophisticated to test such hypothesis. Both observations (Kodera, 1995; Claud et al., 2008) and numerical simulations (Matthes et al., 2006) have now confirmed this mechanism. When the planetary waves have small amplitudes, they impact weakly the mean flow and consequently the polar vortex is well established, circular and mainly circumpolar, forced radiatively by the polar night conditions. Winds are stronger and the temperatures are the lowest due to the minimum excursion of the vortex over areas receiving sunlight. Conversely, when the wave amplitudes are larger with higher wave numbers, the interactions with the circular flow are stronger, resulting in a perturbed (displaced or elongated) and weakened vortex with many excursions to lower latitudes. Because of more sunlight exposure of the vortex, temperatures are higher, weakening further the vortex. Sometimes, when the zonal flow is highly disturbed, the vortex breaks up for several successive days and temperatures increase drastically, generating SSW events. The associated modifications of the large-scale Brewer–Dobson have also been reported (see the review by Gray et al., 2010). Since the planetary wave activity is much lower in the southern hemisphere than in the northern hemisphere, the response to the solar forcing through the mechanism discussed previously is expected to be weaker in the southern hemisphere than in the northern hemisphere, as it is the case in our model results. However, in the northern winter hemisphere, the atmospheric response is more complex as seen in Figs. 4b, 5b, 6b where large different changes in amplitude and sign occur from month to month. In contrast to the early winter southern hemisphere, in the northern winter hemisphere, the observed response is not only due to a continuous differential effect from solar maximum to minimum conditions in planetary wave forcing but rather due to the occurrence of Sudden Stratospheric Warmings (SSW). SSW, as a triggering mechanism, has been already mentioned and simulated (Hampson et al., 2005) and it has been suggested that the solar forcing could modify the occurrence of SSW (Sonnemann and Grygalashvyly, 2007; Gray et al., 2001, 2004). In fact the month-to-month variability of the atmospheric response to solar forcing and the modification of the sign of the response can only be understood when investigating the timing of the occurrence of the sudden stratospheric warming rather than the mean absolute winter occurrence. This explanation has been suggested by Gray et al. (2006) in investigating the Solar Cycle/QBO interactions. SSW that are commonly observed in the northern hemisphere in winter correspond to a very spectacular phenomenon that induces large temperature and wind deviation at middle and high latitudes. SSW are, however, a very unstable processes and do not occur each year, not at the same time during the course of the winter and very seldom in the southern hemisphere (Labitzke, 1981). It was for the first time in

2002 that a major warming was detected in the Southern Hemisphere (Baldwin et al., 2003). Generally during early and mid-winter, the westerly circulation develops due to the radiative cooling of the polar stratosphere and the formation of the polar vortex. In the northern hemisphere, extra-tropical planetary waves, formed in the troposphere by the thermal and orographic contrasts between oceans and continents, can propagate upwards in westerly winds (Charney and Drazin, 1961) and grow until they reach a critical amplitude and break, leading to a sudden disruption of the zonal circulation (Matsuno, 1971; Hauchecorne and Chanin, 1983). During a SSW, polar stratospheric temperatures increase by up to 40–60 K in one week at 10 hPa (around 30 km). When a reversal of the zonal-mean wind to an easterly direction is reached at 60°N down to 10 hPa (Labitzke, 1977), these events are qualified as major stratospheric warmings. If they occur at the end of the winter (March–April), they mark the transition between winter westerly winds and summer easterly winds and are qualified as final warmings. Major SSW do not occur in all winters, but are reported nearly every second winter while minor warmings (not leading to a breakdown of the polar vortex) occur 1–2 times every winter (Dunkerton and Baldwin, 1991). A documented climatology of SSW for the period 1958–2002 can be found in Charlton and Polvani (2007).

4.2. Solar response for the northern hemisphere winter

To better understand the role of the SSW in the stratospheric response to solar forcing, Figs. 7b and 8b present the seasonal evolution of temperature at 90°N, 10 hPa and zonal wind at 60°N, 10 hPa respectively. These figures show that in the northern hemisphere, winter temperature and zonal wind exhibit a large variability in both minimum and maximum solar conditions. In 48% of the winters (24 over 50), a major warming occurs in the model between mid-November and mid-March according to WMO criteria on polar temperature and wind at 60°N. This compares well with observations: Labitzke and Kunze (2009) indeed report 41% of winters (28 over 68 from 1942 to 2009) with a mid-winter major warming. Significant mean differences can be observed between solar minimum and maximum conditions (Figs. 7b and 8b) with large month to month fluctuations. During solar minimum conditions, early winter (November–December) shows a few SSW followed by relatively cold temperature and strong zonal wind, while mid-winter usually warms progressively through warming events and few cold late winters. Temperatures during solar maximum conditions exhibit a larger variability with a tendency to induce SSW already from December. After the SSW, the blocking of planetary wave upward propagation by easterly

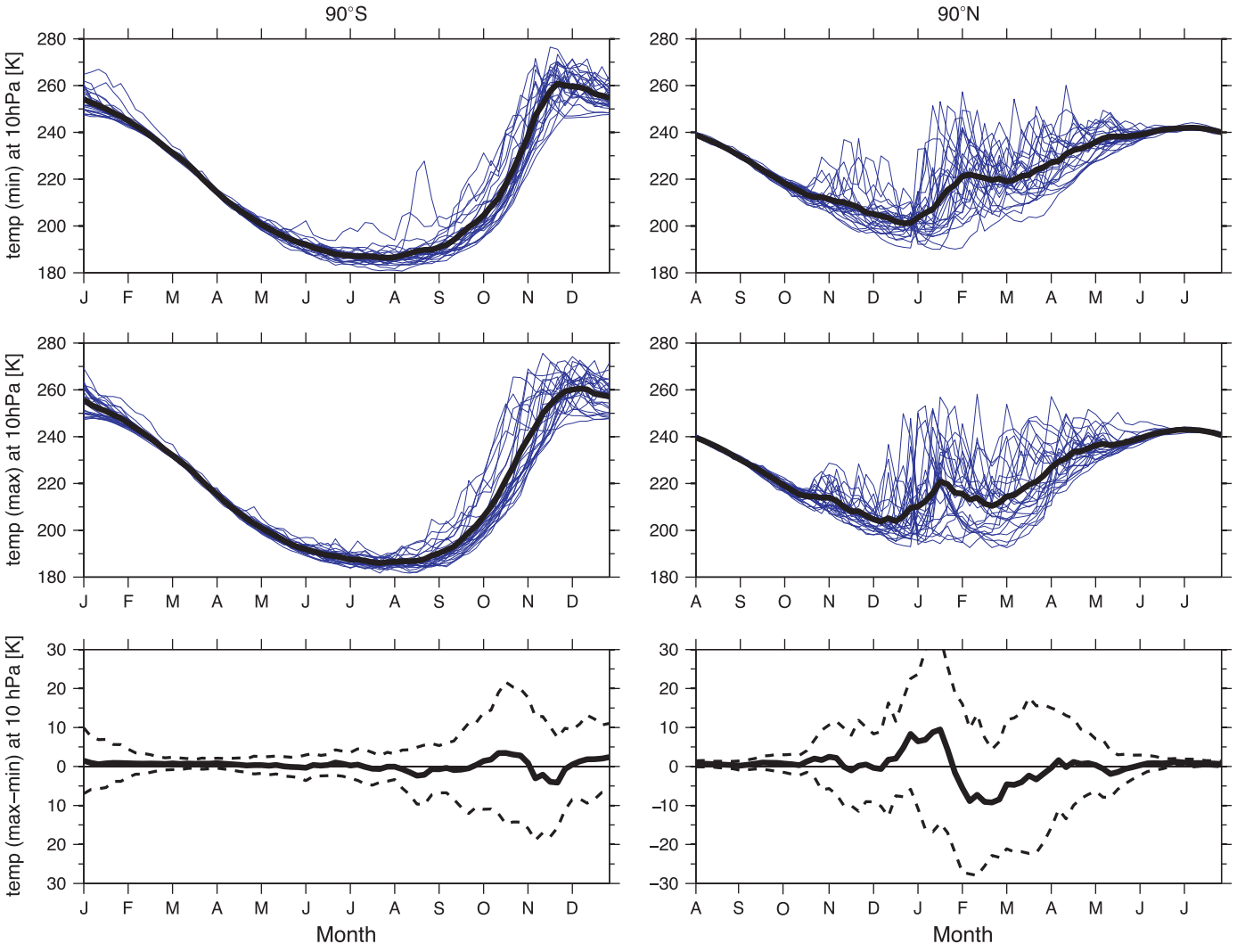

Fig. 7. Monthly temperature evolution at 90°S (left) and 90°N (right) from the LMDz-Reprobus simulations. The 26 years of simulations are represented in blue and the monthly climatology of these simulations in black for the solar minimum (top), solar maximum (middle) conditions and the differences (max-min) (bottom). Dashed line corresponds to the variance of the difference. (For interpretation of the references to color in this figure legend, the reader is referred to the web version of this article.)

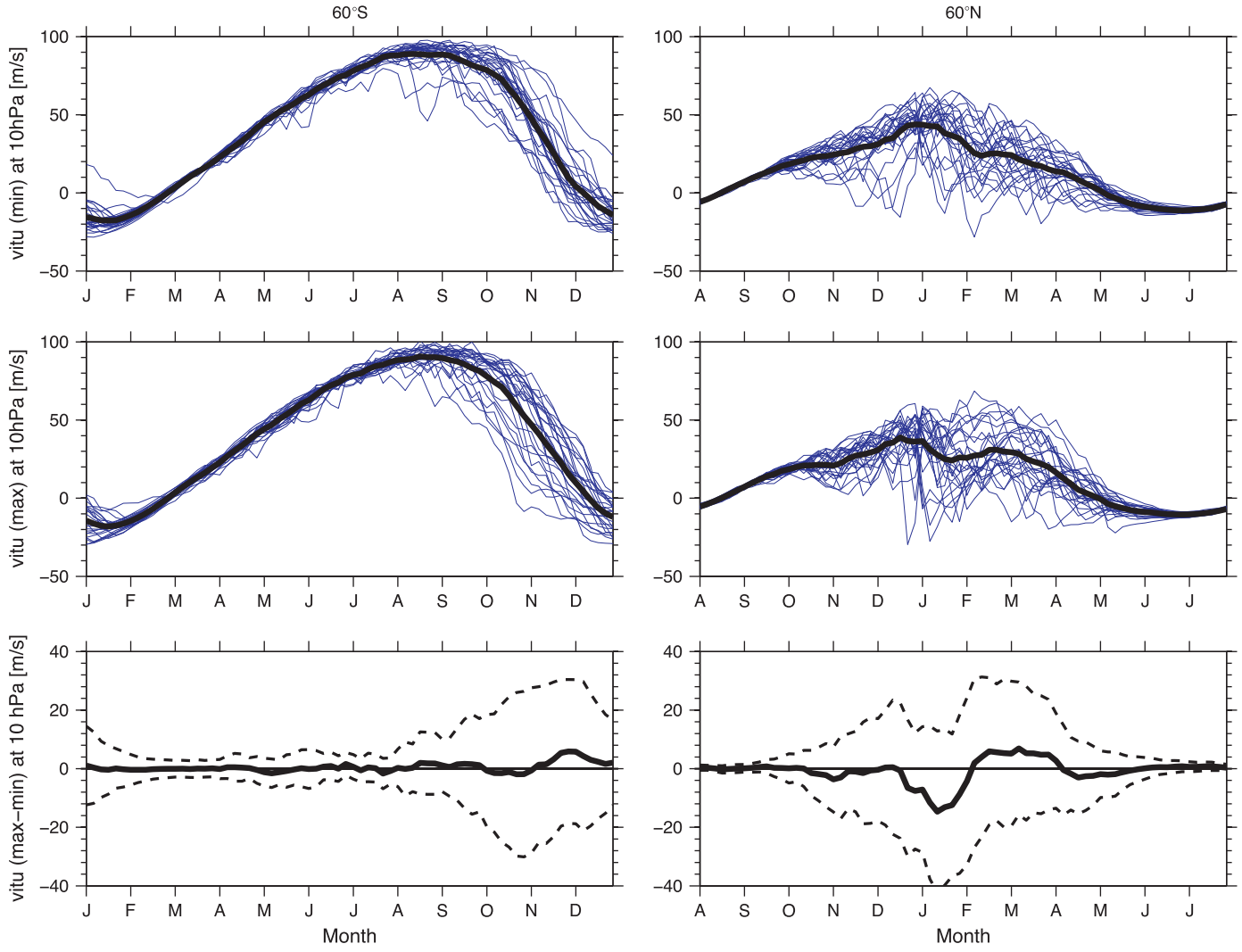

Fig. 8. Same as Fig. 6 but for monthly zonal winds at 60°S (left) and 60°N (right).

wind allows the vortex to radiatively cool in February–March and a strong final warming occurs in April reaching similar temperatures than solar minimum conditions. Winds reveal also alternative structure associated with successive differential polar vortex conditions (Fig. 8b). In the mesosphere, anti-correlated temperatures are observed as shown by Matsuno (1971) and Keckhut et al. (2012) due to the balance of the global circulation.

4.3. Solar response for the southern hemisphere winter

A large hemispheric difference is observed due to the well known difference on Planetary Wave (PW) activity and interaction with the mean flow leading to a globally stronger vortex than in the northern hemisphere. During the southern hemisphere winter for solar maximum conditions, a stronger polar jet and cooler vortex is observed (Figs. 7a and 8a) but the differences are hardly statistically significant. This is probably due to statistically weaker wave activity, providing best conditions to enhance the vortex stability. In late winter, temperature and wind vertical profiles show alternate features likely due to the timing of the final breakdown of the vortex. On average, the vortex breakdown for solar minimum conditions occurs earlier, probably related to its weakness.

4.4. Interactions between ozone, temperature, wind and planetary waves in the northern hemisphere

Ozone responds differently to these dynamical disturbances according to the dominant mechanism of photodissociation versus transport and dynamics. When photochemical equilibrium dominates, from around 30 to 70 km, the well-known anti-correlation between ozone and temperature is observed through the temperature dependence of the oxygen/ozone equilibrium (Rood and Douglass, 1985). In the lower part of the atmosphere, the atmosphere is mainly controlled by dynamical processes (Garcia and Solomon, 1990). As a result, ozone changes are expected to be driven by the wind changes, either horizontal or vertical at different scales (Rood and Douglass, 1985; Gibson-Wilde et al., 1997), and hence the relationship between ozone and temperature is more complex (Wang et al., 1983). While the largest atmospheric response to solar forcing is observed in the stratospheric high latitudes and is due to planetary wave propagation and SSW, the mean winter evolution appears to be better trapped by using time sampling of 10 days as in Matthes et al. (2006). The wind evolution over 10-day periods reveals fluctuations (Fig. 9) that are due to the mean wave interactions and successive SSW. For different solar conditions, the mean timing of the dynamical disturbances associated with SSW differs and leads to large solar signals in wind and temperature.

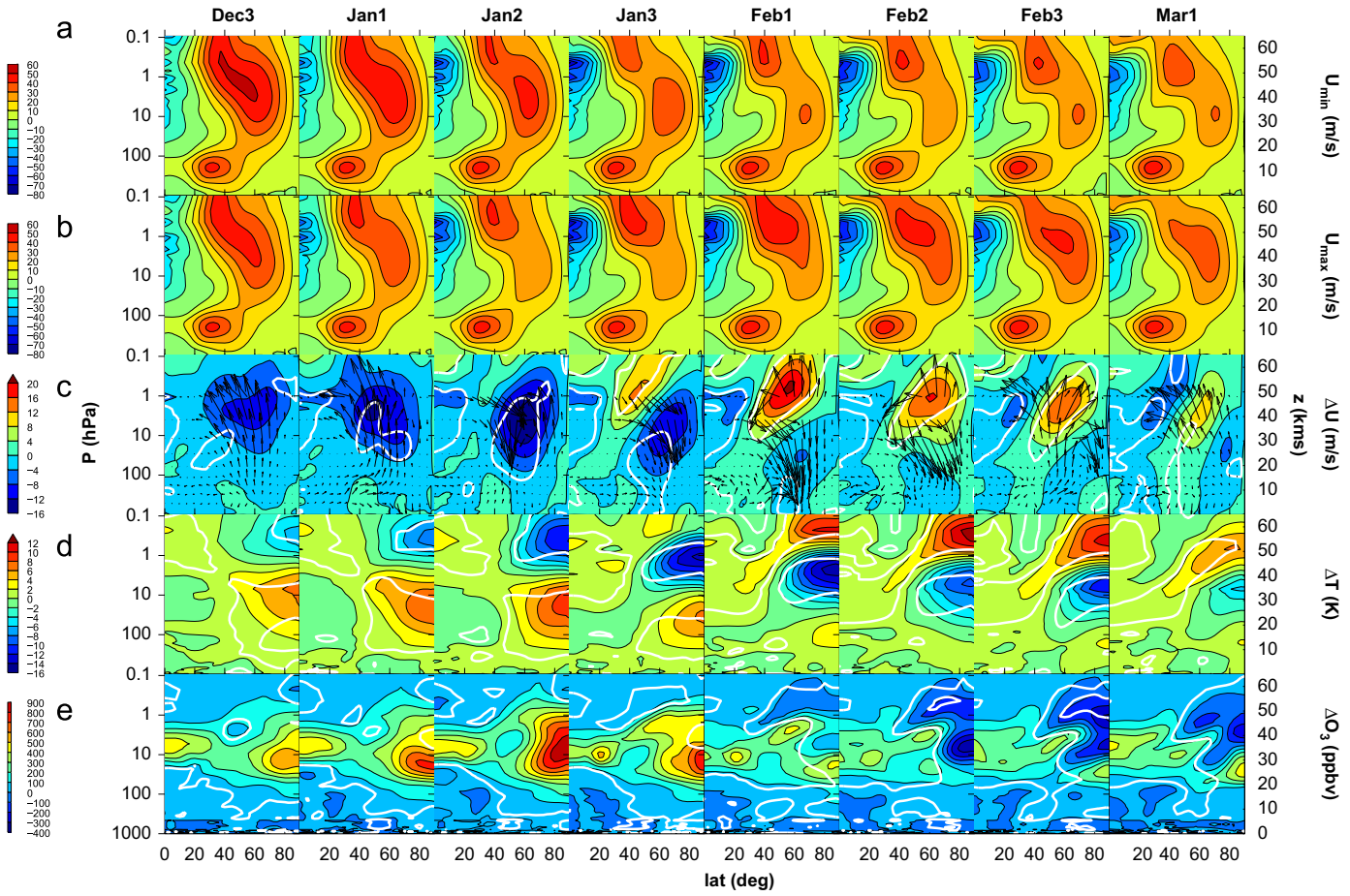

Fig. 9. (a) Long-term 10-day mean of the zonal wind *vitu* for the run in minimum of activity for the NH from Dec3 to Mar1 (Dec3 = 3rd 10-day period of December and Mar1 = 1st 10-day period of March). (b) Mean zonal wind *vitu* in maximum of activity for the NH from Dec3 to Mar1. (c) Zonal wind differences between the minimum and maximum experiments and long-term 10-day mean differences of the Eliassen-Palm Flux vector (EPF) vector (arrows, scaled by the inverse of pressure to highlight the changes in the upper stratosphere) for the NH from Dec3 to Mar1. (d) Zonal mean temperature differences *temp*. Thin white lines indicates the 95% significance level calculated with a Student's *t*-test. Note that *z* is an approximate altitude computed from the pressure *p* with a constant scale height of 7 km.

In early winter, both the UV increase and the induced stratospheric ozone enhancement (Fig. 9e) lead to a direct stratospheric tropical warming around 1 m hPa (Fig. 9d). The velocity and direction of the planetary waves are then modified as it clearly appears in December and early January (Fig. 9c). The large wave activity observed at the beginning of the winter during the solar maximum conditions, represented by the Eliassen-Palm Flux vector (EPF), leads to a stronger wave mean flow interaction and reduces the zonal wind at mid-latitudes (30°–70°) in the upper stratosphere (30–50 km) in January, while for the same period, the zonal wind during solar minimum conditions, remains stronger. In mid-January (JAN2) where most of the stratospheric warmings occur during solar max conditions, the wind decreases (14 m/s), the induced warming in the lower stratosphere (9 K) and associated cooling in the mesosphere (11 K) are the largest compared to solar min conditions. Ozone mixing ratio (Fig. 9e) increases at all altitudes between 15 and 50 km. This corresponds to a correlation with temperature below 40 km where ozone evolution is controlled by the dynamics, the SSW bringing tropical air rich in ozone to polar latitudes, and an anti-correlation above 40 km explained by the temperature dependent photochemical equilibrium of ozone at this altitude. Planetary waves propagating from the mid-latitude troposphere upward to the stratosphere are then refracted at proximity of the west wind anomaly appearing during mid-January (JAN2) (Fig. 9c) and well represented also by the anomalous positive anomaly of the EPF acceleration divergence during the same month (not shown here). Those solar signatures, while located during one month, are statistically significant (> 95%).

During solar min conditions, the slower development of wave activity in the stratosphere in the early winter is associated with a well established polar vortex in mid-winter and a greater probability of conditions favourable to late SSW occurrence. In this simulation, stratospheric warmings start to appear in January with a maximum in early February, as shown by the temporal evolution of the 10-days mean wind (Fig. 9a). During the same period, solar max conditions exhibit a reinforced vortex after the stratospheric warming period, and an associated damped planetary wave activity. Thus waves dissipate at lower altitudes and decelerate the zonal mean wind in the mid-latitude upper stratosphere as shown by the relative easterly winds and convergence of the EP flux in late January. Concurrently, a negative anomaly of the zonal wind appears in the tropical band, develops and migrates poleward in February, while the positive anomaly shifts further downward in the lower stratosphere.

The resulting differences between the two solar conditions are then maximum in early February. A zonal mean wind difference of 20 m/s can be noted around the stratopause of the mid-latitudes (60°) and significant temperature differences of more than 10 K in the upper stratosphere and lower stratosphere with an opposite sign, and wave activity as described by EPF, are larger during solar minimum. During the transition period in late January and early February, the bimodal thermal structure and the wind difference seem to show a downward shift of the

response pattern as already reported by previous studies (Kodera and Kuroda, 2002; Matthes et al., 2006). These features result from the fact that stratospheric warmings tend to start earlier during solar max conditions and appear first in the upper stratosphere.

In comparison to Matthes et al. (2006), our results are similar but shifted in time by about 1–2 months. This may be due to the fact that first, in the runs of Matthes et al. (2006), ozone changes are prescribed whereas ozone is computed interactively in our LMDZ-Reprobus model, and second, they used prescribed QBO-like winds whereas no QBO (Quasi-Biennal Oscillation) is included in our model.

4.5. Comparisons with observations

Comparisons with observations are not easy mostly because the reported stratospheric response to solar forcing depends on the QBO (Labitzke, 2007; Matthes et al., 2010; Salby and Callaghan, 2000), which is not represented in our model. During the West QBO phase, highly positive correlations of the zonally averaged temperature in the lower stratosphere with the solar signal are observed. These high correlations are associated with the fact that more SSW are observed for solar maximum, inducing a positive temperature difference between solar maximum and solar minimum peaking in February when the planetary wave activity is found to be largest (Van Loon and Labitzke, 2000). During the East QBO phase, a weaker and less significant negative response is observed. These negative correlation is connected to the frequent occurrence of SSW at solar minima. Although the QBO is not represented in LMDz-Reprobus, the equatorial zonal wind is more representative of East QBO phase with dominant easterly winds in the whole stratosphere. The negative response in February in the model is in agreement with the weak negative response during the East phase observations (Labitzke, 2007). The time of occurrence of SSW in the winter is more reproducible in the model, with preferred periods on both solar minimum and solar maximum than in observations where SSW are observed all around the winter. This may be due to the use of a prescribed SST annual cycle. The difference between solar maximum and solar minimum conditions in the model is clearly related to the difference in the development of Planetary Wave (PW) activity in early winter. Further studies are needed to understand why PW develop more for solar maximum conditions in early winter and why SSW start to occur earlier in the model than in observations. This latter point cannot be considered as a model artefact, since according to the SPARC-CCM Val Report (2011, Chapter 4), the representation of SSW in LMDz-Reprobus is rather realistic both in terms of frequency (albeit slightly more SSWs than in reanalyses, see Fig. 4.25) and timing (Fig. 4.26). Compared to other models, the development of SSWs in early winter is generally less frequent in LMDz-Reprobus.

5. Longitudinal response

Because the mechanisms that explain the mid- and high-latitudes winter solar signature in the northern hemisphere involve SSW, the zonal nature of the signature can be questionable. Stratospheric warmings induce vortex disturbances in mainly two classes: elongated vortex splitting into two pieces, or a vortex displacement characterized by a clear shift of the polar vortex off the pole, and its subsequent distortion into a “comma shape” (Labitzke, 1981). The longitudinal evolution of the temperature differences associated with the geopotential heights difference at 10 hPa for both selected periods of mid January (JAN2) and mid February (FEB2) is represented in Fig. 10. Apart from the clear reversal of the anomaly of temperature above the Arctic already visible in Fig. 9, we observe a clear longitudinal asymmetry specially above Europe and North America where it is warmer for solar maximum than above Asia

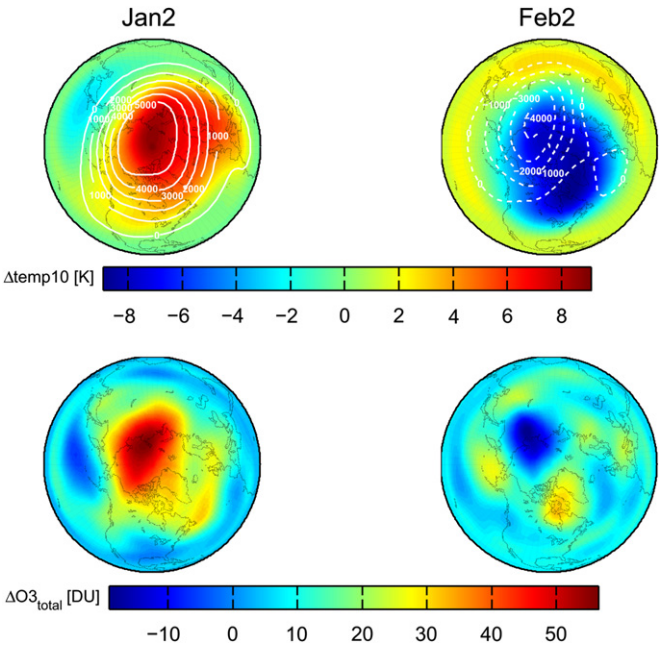

Fig. 10. Polar projection from 0° to 90° of the long-term 10-day mean differences of the temperature at 10 hPa and ozone column between the solar maximum and minimum experiments in Jan2 and Feb2. Also plotted in white the contour of the difference of the geopotential heights at the same pressure level. Contour interval: 1000 m^2/s^2.

where it tends to be colder in mid-January (JAN2). This asymmetry tends to reverse in mid-February (FEB2) where this becomes colder at this level pressure above Europe and North America. The contour of the geopotential height difference at 10 hPa shows a clear positive anomaly at the pole in mid-January (JAN2) getting negative in mid-February (FEB2) corresponding to a stronger polar vortex in maximum of activity due to a stronger Polar Night Jet (PNJ). Both patterns are very similar. The signature is barotropic in January with a good correspondence between positive anomalies in temperature and geopotential height and is more baroclinic in February with a displacement of the maximum of negative signature shifted toward East Siberia in geopotential height. Such non-zonal effect confirms the preliminary finding obtained with a mechanistic model (Hampson et al., 2005). The total ozone difference in January (Fig. 10) presents a maximum positive value above Arctic and North Siberia of up to 50 Dobson Units (DU) in phase with temperature and geopotential height differences. This very large anomaly is explained by the fact that the ozone difference is positive in the whole stratosphere. In February a negative total ozone difference is observed above North Siberia, in phase with the geopotential height. It is surrounded by several regions with a positive difference. These results suggest that data analysis should be performed on sampling periods compatible with SSW timescales (typically over 10-day periods) and regionally instead of considering monthly or seasonal zonal means. A comprehensive understanding of the impact of the 11-year solar cycle on the atmosphere requires to consider zonally asymmetric ozone as an additional intermediary for communicating variations in solar cycle to the atmosphere through wave-mean flow interaction (Nathan et al., 2011).

6. Discussion

In this paper, results from the CCM LMDz-Reprobus simulations have been considered to investigate the dynamical amplification of the stratospheric solar response to the 11-year solar cycle.

The present study is focused on the dynamical relationship between the stratospheric solar response and the occurrence of stratospheric warmings and their timing using analyses of monthly and 10 days mean model outputs, particularly at high latitudes. Overall, the annual mean response clearly shows a radiative and photochemical response, especially in the upper stratosphere, while the monthly analysis presented in this paper suggests the importance of the dynamical response, as already reported in observations (Chandra, 1986; Keckhut et al., 2005; Claud et al., 2008). Our results emphasize the crucial role of stratospheric circulation changes in middle and high latitudes. Our study supports the mechanism proposed by Kodera and Kuroda (2002) by which modifications in the winter polar stratosphere brought about by anomalous solar heating may influence the upward propagation of planetary waves and thus their deposition of momentum involved in the strength of the mean stratospheric overtuning. The main temperature and wind responses are due to a statistically different timing of the occurrence of SSW according to systematic small changes of the planetary wave propagation induced by the solar conditions. Successive positive and negative responses are then reported during the course of the winter, showing some consistencies with the observations in the upper stratosphere-lower mesosphere as shown in Keckhut et al. (2005). In the model, solar minimum conditions are generally associated with a stronger vortex in early winter while solar maximum conditions experience more early SSW, as illustrated by a stronger wave mean flow interaction and reduced zonal wind at mid-latitudes in the upper stratosphere. The study by Kodera et al. (2003), which investigated the relationship between the interannual variation of the winter atmosphere and the solar forcing, showed that the solar response moves from a radiatively driven stage to a dynamically driven stage through a transition period. This regime-like structure can produce a large dynamical response to the initial solar forcing, with the variations in wave forcing being possibly produced by the changes in the propagating conditions in the stratosphere. Our work, which investigated more precisely the second stage of this process, provides further evidence for this mechanism, at least in our model. In February, the solar–atmospheric response is opposite because the solar minimum conditions induce some SSW while solar maximum conditions exhibits a reinforced vortex after the stratospheric warming period, and damped planetary wave activity. In late winter, a reversal of temperature differences is obtained with major SSW mostly observed during solar maximum conditions. This agrees with SSW occurrence studies based on meteorological reanalyses that reveal a different timing of SSW according to solar conditions (Gray et al., 2004; Camp and Tung, 2007). Our results confirm those reported in a previous publications, even if they are shifted in time. Whether this shift can be explained by the specific behaviour or biases of our model or by the differences in the runs (prescribed versus interactive ozone and prescribed versus no QBO) remains to be assessed. However, as pointed above, no bias towards a too large development of SSW in early winter has been found in LMDz-Reprobus (SPARC-CCM Val Report, 2011, Chapter 4). In the southern hemisphere, the largest winter solar signal consists in an enhanced and more persistent vortex during solar maximum conditions. At the end of the winter too, some alternated features can be observed due to a shift of the timing of the final warming.

As a summary, our study demonstrates that:

1. The stratospheric response to solar forcing is very variable in time from month to month, and even at shorter timescales, and regionally due to the non-zonal nature of SSW ; this has strong implications in the way of analyzing observational data through the choice of the averaging processes. It is therefore recommended to avoid multi-months and/or zonal data averaging to characterize the solar response in the northern hemisphere at mid and high latitudes.
2. The term dynamical amplification used in the text does not imply a systematic global mean warming or cooling (none of them is reported here), but rather a significant spatio-temporal redistribution of the energy momentum leading to detectable solar signals in some regions for specific periods in the stratosphere. A similar variability of the response in the troposphere is also possible. Since large stratospheric solar signals have been reported here, changes in ozone distribution and in stratospheric warmings occurrence can be seen as a two-step amplification mechanism of the direct irradiance solar forcing. Ozone production (almost entirely due to the photolysis of O_2 in the UV range in the stratosphere) is very sensitive to the UV solar spectrum modifications, and SSWs are a triggering mechanism that is very sensitive to changes in the background wave propagating conditions. Therefore, even small changes in the solar UV can impact the ozone distribution, resulting in modifications of the temperature latitudinal gradients and zonal wind intensity. Subsequently, small changes in zonal wind can be sufficient to generate SSWs.
3. The ground response is expected to be non zonal at least as much as the stratospheric response is concerned. Our understanding of stratosphere–troposphere dynamical coupling needs to be improved to understand the ground response through a downward propagation of the signal. A comprehensive understanding of the impact of the 11-year solar cycle on the atmosphere requires to consider zonally asymmetric ozone as an additional intermediary for communicating variations in solar cycle to the atmosphere through wave-mean flow interaction (Nathan et al., 2011). It is, however, clear that only CCM coupled with an ocean model can provide a realistic climate response at the surface, with the ocean contributing to complexify the regional variability of the response, e.g. Rind et al. (2008) and Meehl et al. (2009).

Finally, these simulated winter features are difficult to compare in detail with observations for several reasons:

First, most of the rare statistical analysis of observations averaged the winter data over a minimum of three months to produce significant statistical results. This study shows a non-uniform response during winter with large alternating features which were suspected in monthly wind analyses performed by Kodera and Kuroda (2002).

The second reason is related to the model forcing. While the model has its own variability and the dynamical parameters exhibit realistic amplitudes, the perpetual prescribed SST cannot induce any forced winter behaviour. These results suggest to use transient simulations instead of the differences between two perpetual annual conditions and a detailed evaluation of the dynamics using Chemistry Transport Models to figure out those who provide the most similar statistical dynamical evolution. An additional caveat of our study is related to the fact that this model does not include the Quasi Biennal Oscillation (QBO). Its is known that this wind oscillation has a strong impact on planetary waves propagation (Holton and Tan, 1980), and so, should also influence the atmospheric solar responses (Kodera, 1991; Labitzke, 2005; Lu et al., 2009).

7. Conclusions

This present modelling study shows that the large temperature responses of the middle atmosphere at mid- and high-latitudes are due to planetary wave propagation and associated stratospheric warming events through two slightly different mechanisms in both hemispheres. In the northern hemisphere, changes are mainly associated with the occurrence of SSW and

their timing along the winter. The temperature changes over the tropics, induced by ozone changes and the level of solar UV emission, impact planetary waves propagation. During solar minimum conditions, simulations indicate a slightly stronger polar vortex in early winter and late SSW, while during solar maximum conditions, earlier SSW can be noted. Large atmospheric responses according to solar activity, with changing signs of the response during the winter, are then reported. In the southern hemisphere, the solar response is less variable and more continuous along the winter only due to planetary wave propagation as no SSW are generated. The largest responses occur at the end of the winter due to the timing of the wind reversal.

This work is a mechanistic approach that needs further investigations to provide a realistic response that can be compared with the solar response and its timing in the observation as the self generation of SSW in Chemistry Climate Models is quite different from one model to another. In this respect, the radiative forcing can be improved but this will not significantly change the mechanism described here. However, if the timing of the response needs to be further investigated, this study shows that the origin of the large temperature changes observed in the stratosphere at mid and high latitudes is better understood and gives some indications about how data should be analyzed in the future to better describe the solar response: averaged over continental regions and by monthly or even 10-day period means rather than for zonal bands and yearly means.

Acknowledgments

This work have been performed within the framework of the Picard space mission. We acknowledge the pole de modelisation team of the IPSL institut. This work was supported in part by grants from the Centre d'Etude spatiale (CNES), from the Agence Nationale de la Recherche (ANR-STTCLIM) and from the European project RECONCILE.

References

Austin, J., Hood, L.L., Soukharev, B.E., 2007. Solar cycle variations of stratospheric ozone and temperature in simulations of a coupled chemistry-climate model. Atmospheric Chemistry and Physics 7, 1693–1706.

Austin, J., et al., 2008. Coupled chemistry climate model simulations of the solar cycle in ozone and temperature. Journal of Geophysical Research 113. doi:10.1029/2007JD009391.

Baldwin, M., Hirooka, T., O'Neil, A., Yoden, S., 2003. Major stratospheric warming in the Southern Hemisphere in 2002: Dynamical aspects of the ozone hole split. SPARC Newsletter 20, 24–26.

Bekki, S., Toumi, R., Pyle, J.A., 1993. Role of sulphur photochemistry in tropical ozone changes after the eruption of Mount Pinatubo. Nature 362, 331.

Brasseur, G., 1993. The response of the middle atmosphere to long-term and short-term solar variability: a two dimensional model. Journal of Geophysical Research 98, 23079–23090.

Camp, C.D., Tung, K.K., 2007. The influence of the solar cycle and QBO on the late-winter stratospheric vortex. Journal of the Atmospheric Sciences 64, 1267–1283.

Chandra, S., 1986. The solar and dynamically induced oscillation in the stratosphere. Journal of Geophysical Research 91, 2719–2734.

Charlton, A.J., Polvani, L.M., 2007. A new look at stratospheric sudden warming events: Part I. Climatology benchmarks. Journal of Climate 20, 449–469.

Charney, J.G., Drazin, P.G., 1961. Propagation of planetary scale disturbances from the lower into the upper atmosphere. Journal of Geophysical Research 66, 83–109.

Claud, C., Cagnazzo, C., Keckhut, P., 2008. The effect of the 11-year solar cycle on the temperature in the lower stratosphere. Journal of Atmospheric and Solar-Terrestrial Physics 70, 2031–2040.

Dunkerton, T.J., Baldwin, M.P., 1991. Quasi-biennal modulation of planetary wave fluxes in the Northern Hemisphere winter. Journal of the Atmospheric Sciences 48, 1043–1061.

Egorova, T., Rozanov, E., Manzini, E., Haberreiter, M., Schmutz, W., Zubov, V., Peter, T., 2004. Chemical and dynamical response to the 11-year variability of the solar irradiance simulated with a chemistry-climate model. Geophysical Research Letters 31, L06119. doi:10.1029/2003 GL019294.

Emanuel, K.A., 1991. A scheme for representing cumulus convection in large-scale models. Journal of the Atmospheric Sciences 48, 2313–2335.

Emanuel, K.A., 1993. A cumulus representation based on the episodic mixing model: the importance of mixing and microphysics in predicting humidity. AMS Meteorological Monographs 24 (46), 185–192.

Eyring, V., Chipperfield, M.P., Giorgetta, M.A., Kinnison, D.E., Manzini, E., Matthes, K., Newman, P.A., Pawson, S., Shepherd, T.G., Waugh, D.W., 2008. Overview of the CCMVal Reference and sensitivity simulations in support of upcoming one and climate assessments and the planned SPA RC CCMVal. SPARC Newsletter 30, 20–26.

Floyd, L.E., Cook, J.W., Herring, L.C., Crane, P.C., 2003. SUSIM's 11-year observational record of the solar UV irradiance. Advances in Space Research 31, 2111–2120 (Record of the solar UV irradiance).

Forster, P.M., Fomichev, V.I., Rozanov, E., Cagnazzo, C., Jonsson, A.I., Langematz, U., Fomin, B., Iacono, M.J., Mayer, B., Mlawer, E., Myhre, G., Portmann, R.W., Akiyoshi, H., Falaleeva, V., Gillett, N., Karpechko, A., Li, J., Lemennais, P., Morgenstern, O., Oberlnder, S., Sigmond, M., Shibata, K., 2011. Evaluation of radiation scheme performance within chemistry climate models. Geophysics Research 116, D10302.

Fouquart, Y., Bonnel, B., 1980. Computations of solar heating of the Earth's atmosphere: a new parametrization. Contributions to Atmospheric Physics 53, 35–62.

Garcia, R.S., Solomon, S., 1990. The effect of breaking gravity waves on the dynamics and chemical composition of the mesosphere and lower thermosphere. Journal of Geophysical Research 90, 3850–3868.

Gibson-Wilde, D.E., Vincent, R.A., Souprayen, C., Godin, S., Hertzog, A., Eckermann, S.D., 1997. Dual lidar observations of mesoscale fluctuations of ozone and horizontal winds. Geophysical Research Letters 24, 1627–1630.

Gray, L.J., Beer, J., Geller, M., Haigh, J.D., Lockwood5, M., Matthes, K., Cubasch, U., Fleitmann, D., Harrison, G., Hood, L., Luterbacher, J., Meehl, G.A., Shindell, D., van Geel, B., White, W., 2010. Solar influences on climate. Reviews in Geophysics 48, RG4001.

Gray, L.J., Rumbold, S.T., Shine, K.P., 2009. Stratospheric temperature and radiative forcing response to 11-year solar cycle changes in irradiance and ozone. Journal of the Atmospheric Sciences 66, 2402–2417.

Gray, L.J., Crooks, S.A., Palmer, M.A., Pascoe, C.L., Sparrow, S., 2006. A possible transfer mechanism for the 11-year solar cycle to the lower stratosphere. Space Science Reviews 125 (1–4), 357–370.

Gray, L.J., Crooks, S.A., Pascoe, C., Sparrow, S., 2004. Solar and QBO influences on the timings of stratospheric sudden warmings. Journal of the Atmospheric Sciences 61, 2777–2796.

Gray, L.J., Phipps, S.J., Dunkerton, T.J., 2001. A data study of the influence of the equatorial upper stratosphere on northern-hemisphere stratospheric sudden warmings. Quarterly Journal of the Royal Meteorological Society 127, 1985–2004.

Haigh, J.D., 1994. The role of stratospheric ozone in modulating the solar radiative forcing of climate. Nature 370, 544–546.

Haigh, J.D., 1999. A GCM study of climate change in response to the 11-year solar cycle. Quarterly Journal of the Royal Meteorological Society 125, 871–892.

Haigh, J.D., 2003. The effects of solar variability on the Earth's climate. Philosophical Transactions of the Royal Society of London 361, 95–111.

Haigh, J.D., 2007. The sun and the earths climate. Living Reviews in Solar Physics 4.

Haimberger, L.C., Tavolato, C., Sperka, S., 2008. Towards elimination of the warm bias in historic radiosonde temperature records—some new results from a comprehensive intercomparison of upper air data. Journal of Climate 21, 4587–4606.

Hampson, J., Keckhut, P., Hauchecorne, A., Chanin, M.L., 2006. The effect of the 11-year solar-cycle on the temperature in the upper-stratosphere and mesosphere Part III: investigations of zonal asymmetry. Journal of Atmospheric and Solar-Terrestrial Physics 68, 1591–1599.

Hampson, J., Keckhut, P., Hauchecorne, A., Chanin, M.L., 2005. The 11-year solar-cycle in the temperature in the upper-stratosphere and mesosphere: Part II numerical simulation and role of planetary waves. Journal of Atmospheric and Solar-Terrestrial Physics 67, 948–958. doi:10.1016/j.jastp.2005.03.005.

Hassler, B., Bodeker, G.E., Cionni, I., Dameris, M., 2009. A vertically resolved, monthly mean ozone database from 1979 to 2100 for constraining global climate model simulations. International Journal of Remote Sensing 30, 4009–4018.

Hauchecorne, A., Chanin, M.L., 1983. Mid-latitude lidar observations of planetary waves in the middle atmosphere during the winter of 1981–1982. Journal of Geophysical Research 88, 3843–3849.

Hines, C.O., 1974. The Upper Atmosphere in Motion: A Selection of Papers with Annotation. Geophysical Monograph, vol. 18, American Geophysical Union.

Holton, J.R., Tan, H.C., 1980. The influence of the equatorial quasi-biennial oscillation on the global circulation at 50 mbar. Journal of the Atmospheric Sciences 37, 2200.

Hood, L.L., Soukharev, B.E., 2003. Quasi-decadal variability of the tropical stratosphere: the role of extratropical wave forcing. Journal of the Atmospheric Sciences 60, 2389–2403.

Hourdin, F., Musat, I., Bony, S., Braconnot, P., Codron, F., Dufresne, J.-L., Fairhead, L., Filiberti, M.-A., Friedlingstein, P., Grandpeix, J.-Y., Krinner, G., LeVan, P., Li, Z., Lott, F., 2006. The LMDZ4 general circulation model: climate performance and sensitivity to parametrized physics with emphasis on tropical convection. Climate Dynamics 27, 787–813.

Jourdain, L., Bekki, S., Lott, F., Lefèvre, F., 2008. The coupled chemistry-climate model LMDz-REPROBUS: description and evaluation of a transient simulation of the period 1980–1999. Annales Geophysicae 26, 1391–1413.

Kanamitsu, M., Ebisuzaki, W., Woollen, J., Yang, S.K., et al., 2002. NCEP-DOE AMIP-II reanalysis (R-2), Bulletin of the American Meteorological Society.
Keating, G.M., Pitts, M.C., Brasseur, G., De Rudder, A., 1987. Response of middle atmosphere to short-term solar ultraviolet variations: 1 Observation. Journal of Geophysical Research 92, 889–902.
Keckhut, P., Hauchecorne, A., Kerzenmacher, T., Angot, G., 2012. Modes of variability of the vertical temperature profile of the middle atmosphere at mid-latitude: similarities with solar forcing. Journal of Atmospheric and Solar-Terrestrial Physics 75–76, 92–97.
Keckhut, P., Cagnazzo, C., Chanin, M.-L., Claud, C., Hauchecorne, A., 2005. The 11-year solar-cycle effects on the temperature in the upper-stratosphere and mesosphere: Part I: assessment of observations. Journal of Atmospheric and Solar-Terrestrial Physics 67, 940–947.
Kodera, K., 1991. The solar and equatorial QBO, influences on the stratospheric circulation during the early Northern Hemisphere winter. Geophysical Research Letters 18, 1023–1026.
Kodera, K., 1995. On the origin and nature of the interannual variability of the winter stratospheric circulation in the Northern Hemisphere. Journal of Geophysical Research 100, 14,077–14,087.
Kodera, K., Kuroda, Y., 2002. Dynamical response to the solar cycle. Journal of Geophysical Research 107 (D24), 4749.
Kodera, K., Matthes, K., Shibata, K., Langematz, U., Kuroda, Y., 2003. Solar impact on the lower mesospheric sub-tropical jet: a comparative study with general circulation model simulations. Geophysical Research Letters 30, 1315. doi:10.1029/2002GL016124.
Labitzke, K., 1977. Interannual variability of winter stratosphere in northern hemisphere. Monthly Weather Review 105, 762–770.
Labitzke, K., 1981. Stratosphreic-mesospheric midwinter disturbances: a summary of observed characteristics. Journal of Geophysical Research 86 (C10), 9665–9678.
Labitzke, K., Austin, J., Butchart, N., Knight, J., Takahashi, M., Nakamoto, M., Nagashima, T., Haigh, J., Williams, V., 2002. The global signal of the 11-year solar cycle in the stratosphere: observations and model results. Journal of Atmospheric and Terrestrial Physics 64, 203–210.
Labitzke, K., 2005. On the solar cycle-QBO relationship: a summary. Journal of Atmospheric and Solar-Terrestrial Physics 67, 45–54.
Labitzke, K., 2007. Solar variation and stratospheric response. Space Science Reviews 125, 247–260.
Labitzke, K., Kunze, M., 2009. On the remarkable Arctic winter in 2008/2009. Journal of Geophysical Research 114, D00I02.
Larkin, A., Haigh, J.D., Djavidnia, S., 2000. The effect of solar UV radiation variations on the earth's atmosphere. Space Science Reviews 94, 199–214.
Law, K.S., Plantevin, P.H., Shallcross, D.E., Rogers, H.J., Pyle, J.A., Grouhel, C., Thouret, V., Marenco, A., 1998. Evaluation of modeled O_3 using Measurement of Ozone by Airbus In-Service Aircraft (MOZAIC) data. Journal of Geophysical Research 103, 25721–25737.
Lean, J.L., 1989. Contribution of ultraviolet irradiance variations to changes in the sun's total irradiance. Science 244, 197–200.
Lefèvre, F., Brasseur, G.P., Folkins, I., Smith, A.K., Simon, P., 1994. Chemistry of the 1991–1992 stratospheric winter: three-dimensional model simulations. Journal of Geophysical Research 199, 8183.
Lefèvre, F., Figarol, F., Carslaw, K.S., Peter, T., 1998. The 1997 Arctic ozone depletion quantified from three-dimensional model simulations. Geophysical Research Letters 25 (13), 2425–2428.
Le Treut, H., Li, Z., Forichon, M., 1994. Sensitivity study of the LMD GCM to greenhouse forcing associated with two different cloud water parametrizations. Journal of Climate 7, 1827–1841.
Le Treut, H., Forichon, M., Boucher, O., Li, Z., 1998. Sulfate aerosol indirect effect and CO_2 greenhouse forcing: equilibrium response of the LMD GCM and associated cloud feedbacks. Journal of Climate 11, 1673–1684.
Lott, F., Fairhead, L., Hourdin, F., Levan, P., 2005. The stratospheric version of LMDz: dynamical climatologies, arctic oscillation, and impact on the surface climate. Climate Dynamics 25, 851–868.
Lu, H., Gray, L.J., Baldwin, M.P., Jarvis, M., 2009. Life cycle of the QBO-modulated 11-year solar cycle signals in the northern hemispheric winter. Quarterly Journal of the Royal Meteorological Society 135, 1030–1043.
McCormack, J.P., Siskind, D.E., Hood, L.L., 2007. Solar-QBO interaction and its impact on stratospheric ozone in a zonally averaged photochemical transport model of the middle atmosphere. Journal of Geophysical Research 112. doi:10.1029/2006JD008369.
Madronich, S., Flocke, S., 1999. The role of solar radiation in atmospheric chemistry. In: Boule, P. (Ed.), Handbook of Environmental Chemistry. Springer-Verlag, Heidelberg, pp. 1–26.
Marsh, D.R., Garcia, R.R., Kinnison, D.E., Boville, B.A., Sassi, F., Solomon, S.C., Matthes, K., 2007. Modelling the whole atmosphere response to solar cycle changes in radiative and geomagnetic forcing. Journal of Geophysical Research 112. doi:10.1029/2006JD008306.
Matsuno, T., 1971. A dynamical model of the stratospheric sudden warming. Journal of the Atmospheric Sciences 28, 1479–1494.
Matthes, K., Kodera, K., Haigh, J.D., Shindell, D.T., Shibata, K., Langematz, U., Rozanov, E., Kuroda, Y., 2003. GRIPS solar experiments intercomparison project: initial results. Papers in Meteorology and Geophysics 54, 71–90.
Matthes, K., Kuroda, Y., Kodera, K., Langematz, U., 2006. Transfer of the solar signal from the stratosphere to the troposphere: northern winter. Journal of Geophysical Research 111, D06108.
Matthes, K., Kodera, K., Gray, L., Austin, J., Kubin, A., Langematz, U., Marsh, D., McCormack, J., Shibata, K., Shindell, D., 2007. Report on the First SOLARIS Workshop 4–6 October 2006, SPARC Newsletters, 28.
Matthes, K., Marsh, D., Garcia, R., Sassi, F., Walter, S., 2010. Role of the QBO in modulating the influence of the 11 year solar cycle on the atmosphere forcings. Journal of Geophysical Research 115. doi:10.1029/2009JD013020.
Meehl, G.A., Arblaster, J.M., Matthes, K., Sassi, F., van Loon, H., 2009. Amplifying the pacific climate system response to a small 11-year solar cycle forcing. Science 325, 1114. doi:10.1126/science.1172872.
Minschwaner, K., Anderson, G.P., Hall, L.A., Yoshino, K., 1992. Polynomial coefficients for calculating O_2 Schumann-Runge cross sections at 0.5 cm^{-1} resolution. Journal of Geophysical Research 97, 10103–10108.
Morcrette, J.J., Smith, L., Fouquart, Y., 1986. Pressure and temperature dependence of the absorption in longwave radiation parametrizations. Contributions to Atmospheric Physics 59 (4), 455–469.
Nathan, T.R., Albers, J.R., Cordero, E.C., 2011. Role of wave-mean flow interaction in Sun-Climate connections: historical overview and some new interpretations and results. Journal of Atmospheric and Solar-Terrestrial Physics 73, 11–12. doi:10.1016/j.jastp.2010.12.013.
Randel, W.J., Wu, F., 2007. A stratospheric ozone profile data set for 1979–2005: variability, trends, and comparisons with columns ozone data. Journal of Geophysical Research 112. doi:10.1029/2006JD007339.
Randel, W.J., et al., 2009. An update of observed stratospheric temperature trends. Journal of Geophysical Research 114. doi:10.1029/2008JD010421.
Rind, D., Shindell, D., Perlwitz, J., Lerner, J., Lonergan, P., Lean, J., McLinden, C., 2004. The relative importance of solar and anthropogenic forcing of climate change between the Maunder Minimum and the present. Journal of Climate 17, 906–929.
Rind, D., 2002. The Sun's role in climate variations. Science 94, 1–11.
Rind, D., Lean, J., Lerner, J., Lonergan, P., Leboissitier, A., 2008. Exploring the stratospheric/tropospheric response to solar forcing. Journal of Geophysical Research 113, D24103. doi:10.1029/2008JD010114.
Rood, R.B., Douglass, A.R., 1985. Interpretation of ozone temperature correlations I: theory. Journal of Geophysical Research 90, 5733–5743.
Rozanov, E.V., Schlesinger, M.E., Egorova, T.A., Li, B., Andronova, N., Zubov, V.A., 2004. Atmospheric response to the observed increase of solar UV radiation from solar minimum to solar maximum simulated by the University of Illinois at Urbana-Campaign climate-chemistry model. Journal of Geophysical Research 109. doi:10.1029/2003JD003796.
Sadourny, R., Laval, K., 1984. January and July performance of the LMD general circulation model. In: Berger, A., Nicolis, C. (Eds.), New perspectives in Climate Modeling. , Elsevier, Amsterdam, pp. 173–197.
Sander, S.P., et al., 2006. JPL: 2006 Chemical kinetics and photochemical data for use in atmospheric studies. Evaluation number 15, JPL Publication 06–2, Jet Propulsion Laboratory, Pasadena, CA.
Salby, M., Callaghan, P., 2000. Connection between the solar cycle and the QBO: the missing link? Journal of Climate 13, 2652–2662.
Savage, N.H., Law, K.S., Pyle, J.A., Richter, A., Nüß, H., Burrows, J.P., 2004. Using GOME NO2 satellite data to examine regional differences in TOMCAT model performance. Atmospheric Chemistry and Physics 4, 1895–1912.
Schmidt, H., Brasseur, G.P., 2006. The response of the middle atmosphere to solar cycle forcing in the Hamburg model of the neutral and ionized atmosphere. Space Science Reviews 125, 345–356.
Shindell, D.T., Faluvegi, G., Miller, R.L., Schmidt, G.A., Hansen, J.E., Sun, S., 2006. Solar and anthropogenic forcing of tropical hydrology. Geophysical Research Letters 33, L24706. doi:10.1029/2006GL027468.
Shindell, D.T., Schmidt, G.A., Miller, R.L., Rind, D., 2001. Northern Hemisphere winter climate response to greenhouse gas, ozone, solar, and volcanic forcing. Journal of Geophysical Research 106, 7193–7210.
Shindell, D., Rind, D., Balachandran, N., Lean, J., Lonergan, P., 1999. Solar cycle variability, ozone, and climate. Science 284, 305.
Sonnemann, G.R., Grygalashvyly, M., 2007. The relationship between the occurrence rate of major stratospheric warmings and solar Lyman-alpha flux. Journal of Geophysical Research 112. doi:10.1029/2007JD008718.
SPARC Report on the Evaluation of Chemistry-Climate Models, 2010, Report N, World meteorological Organisation, Geneva, Switzerland.
Stamnes, K., Tsay, S.-C., Wiscombe, W., Jayaweera, K., 1988. Numerically stable algorithm for discrete-ordinate-method radiative transfer in multiple scattering and emitting layered media. Applied Optics 27, 2502–2509.
Thuillier, G., Floyd, L., Woods, T.N., Cebula, R., Hilsenrath, E., Hers, M., Labs, D., 2004. Solar irradiance spectra for two solar activity levels. Advances in Space Research 34, 256–261.
Tiedtke, M., 1989. A comprehensive mass flux scheme for cumulus parametrization in large scale models. Monthly Weather Review 117, 1779–1989.
Tourpali, K., Schurmans, C.J.E., von Dorland, R., Steil, B., Brühl, C., 2003. Stratospheric and tropospheric response to enhanced solar UV radiations: a model study. Journal of Geophysical Research Letters 30, 1231. doi:10.1029/2002GL016650.
Uppala, S.M., et al., 2005. The ERA-40 re-analysis. Quarterly Journal of the Royal Meteorological Society 131, 2961–3012.
Van Loon, H., Labitzke, K., 2000. The influence of the 11-year solar cycle on the stratosphere below 30 km: a review. Space Science Reviews 94, 259–278.
Wang, P.H., Mc Cormick, M.P., Chu, W.P., 1983. A study on the planetary wave transport of ozone during the late February 1979, stratospheric warming using the SAGE ozone observation and meteorological information. Journal of the Atmospheric Sciences 40, 2419–2431.